



Heriot-Watt University  
Research Gateway

## The "quasi-stable" lipid shelled microbubble in response to consecutive ultrasound pulses

### Citation for published version:

Thomas, DH, Butler, M, Anderson, T, Emmer, M, Vos, H, Borden, M, Stride, E, de Jong, N & Sboros, V 2012, 'The "quasi-stable" lipid shelled microbubble in response to consecutive ultrasound pulses', *Applied Physics Letters*, vol. 101, no. 7, ARTN 071601. <https://doi.org/10.1063/1.4746258>

### Digital Object Identifier (DOI):

[10.1063/1.4746258](https://doi.org/10.1063/1.4746258)

### Link:

[Link to publication record in Heriot-Watt Research Portal](#)

### Document Version:

Publisher's PDF, also known as Version of record

### Published In:

Applied Physics Letters

### General rights

Copyright for the publications made accessible via Heriot-Watt Research Portal is retained by the author(s) and / or other copyright owners and it is a condition of accessing these publications that users recognise and abide by the legal requirements associated with these rights.

### Take down policy

Heriot-Watt University has made every reasonable effort to ensure that the content in Heriot-Watt Research Portal complies with UK legislation. If you believe that the public display of this file breaches copyright please contact [open.access@hw.ac.uk](mailto:open.access@hw.ac.uk) providing details, and we will remove access to the work immediately and investigate your claim.

## The “quasi-stable” lipid shelled microbubble in response to consecutive ultrasound pulses

D. H. Thomas, M Butler, T. Anderson, M. Emmer, H. Vos, M. Borden, E. Stride, N. de Jong, and V. Sboros

Citation: [Applied Physics Letters](#) **101**, 071601 (2012); doi: 10.1063/1.4746258

View online: <http://dx.doi.org/10.1063/1.4746258>

View Table of Contents: <http://scitation.aip.org/content/aip/journal/apl/101/7?ver=pdfcov>

Published by the [AIP Publishing](#)

---

### Articles you may be interested in

[Irinotecan delivery by microbubble-assisted ultrasound - A pilot preclinical study](#)

AIP Conf. Proc. **1503**, 40 (2012); 10.1063/1.4769914

[Mechanisms for microvascular damage induced by ultrasound-activated microbubbles](#)

AIP Conf. Proc. **1481**, 41 (2012); 10.1063/1.4757308

[Compare ultrasound-mediated heating and cavitation between flowing polymer- and lipid-shelled microbubbles during focused ultrasound exposures](#)

J. Acoust. Soc. Am. **131**, 4845 (2012); 10.1121/1.4714339

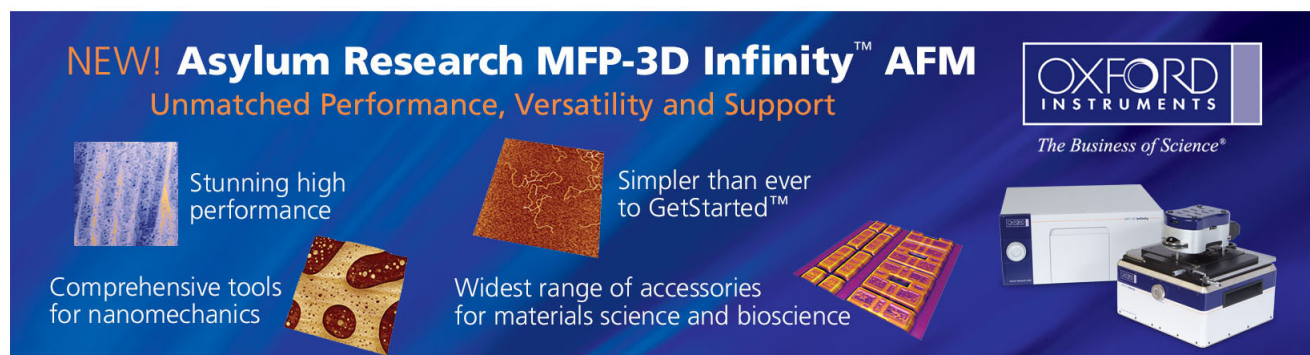
[Chirp excitation technique to enhance microbubble displacement induced by ultrasound radiation force](#)

J. Acoust. Soc. Am. **125**, 1410 (2009); 10.1121/1.3075548

[Characterization and UltrasoundPulse Mediated Destruction of Ultrasound Contrast Microbubbles](#)

AIP Conf. Proc. **838**, 271 (2006); 10.1063/1.2210360

---

The advertisement features a dark blue background with white and orange text. At the top left, it reads 'NEW! Asylum Research MFP-3D Infinity™ AFM' in large white letters, followed by 'Unmatched Performance, Versatility and Support' in orange. On the right, the Oxford Instruments logo is shown with the tagline 'The Business of Science®'. Below the text are several images: a blue textured surface, a brown textured surface, a grid of colorful rectangular samples, and the MFP-3D Infinity AFM instrument itself. Text boxes describe the instrument's capabilities: 'Stunning high performance', 'Simpler than ever to GetStarted™', 'Comprehensive tools for nanomechanics', and 'Widest range of accessories for materials science and bioscience'.

## The “quasi-stable” lipid shelled microbubble in response to consecutive ultrasound pulses

D. H. Thomas,<sup>1(a)</sup> M Butler,<sup>1</sup> T. Anderson,<sup>1</sup> M. Emmer,<sup>2</sup> H. Vos,<sup>2</sup> M. Borden,<sup>3</sup> E. Stride,<sup>4</sup> N. de Jong,<sup>2</sup> and V. Sboros<sup>1,5</sup>

<sup>1</sup>Medical Physics, Centre for Cardiovascular Science, The University of Edinburgh, Edinburgh, United Kingdom

<sup>2</sup>Thorax Centre, Biomedical Engineering, Erasmus Medical Center, Rotterdam, The Netherlands

<sup>3</sup>Department of Mechanical Engineering, University of Colorado, Boulder, Colorado 80309-0427, USA

<sup>4</sup>Institute of Biomedical Engineering, University of Oxford, Oxford, United Kingdom

<sup>5</sup>Institute of Biological Chemistry, Biophysics and Bioengineering, Heriot Watt University, Edinburgh, United Kingdom

(Received 15 May 2012; accepted 2 August 2012; published online 16 August 2012)

Controlled microbubble stability upon exposure to consecutive ultrasound exposures is important for increased sensitivity in contrast enhanced ultrasound diagnostics and manipulation for localised drug release. An ultra high-speed camera operating at  $13 \times 10^6$  frames per second is used to show that a physical instability in the encapsulating lipid shell can be promoted by ultrasound, causing loss of shell material that depends on the characteristics of the microbubble motion. This leads to well characterized disruption, and microbubbles follow an irreversible trajectory through the resonance peak, causing the evolution of specific microbubble spectral signatures. © 2012 American Institute of Physics. [<http://dx.doi.org/10.1063/1.4746258>]

The rapidly developing field of contrast-enhanced ultrasound spans application areas from molecular diagnostics to novel therapeutic techniques.<sup>1,2</sup> The introduction of viscoelastic phospholipid shells to physically stabilise microbubbles over prolonged periods *in vivo*<sup>3</sup> has enabled their safe and reproducible usage as contrast agents in diagnostic ultrasound, as a means to enhance the echogenicity of the blood pool and the microcirculation during ultrasound imaging.<sup>1</sup> In modern diagnostic ultrasound applications, microbubbles are exposed to a series of short ultrasound pulses. Subsequent signal processing enables both tissue scatter cancellation and exploitation of the microbubble nonlinear properties. Their use as drug/gene delivery agents is also attractive, as they can promote (a) site specific targeting,<sup>4</sup> (b) increased cell permeability and membrane permeation,<sup>5</sup> and (c) deliver gene or other drugs safely in a variety of techniques.<sup>6,7</sup> However, the mechanism of ultrasound mediated microbubble disruption and degradation remains unclear<sup>8–10</sup> and this hinders the development of both advanced imaging modalities and efficient drug delivery strategies for an integrated therapeutics approach.

The existing literature suggests that acoustic fields can be controlled to avoid damage to the microbubble shell, which will otherwise irreversibly lose structural integrity above the fragmentation threshold.<sup>11</sup> However, the structural stability, and hence the stability of the backscattered signal, of the microbubble below such a threshold has not been interrogated until recently. New experimental techniques that enable detailed optical observation of the microbubble shell during oscillation hint at physical mechanisms such as buckling,<sup>12,13</sup> lipid shedding<sup>14,15</sup> and deflation,<sup>16</sup> although

the intricacies of ultra high-speed optical experiments limit the sample sizes obtained.

The study of the mechanisms that underlie this “quasi-stable” behaviour of microbubbles over a series of pulses is the aim of the present letter. A high speed optical camera was deployed to examine the response of single microbubbles to ultrasound exposure. Results show that as microbubbles decay they shed shell material and follow an irreversible trajectory through the resonance peak, leading to a well characterized evolution of oscillation amplitude. The amount of material removed from the shell is shown to be dependant upon the relative amount compression during each the oscillation.

Perfluorocarbon-filled phospholipid coated microbubbles (Definity<sup>®</sup>, Lantheus Medical Imaging N. Billerica, MA, USA) were imaged using an ultra-high speed optical camera system. Microbubbles were isolated in solution at room temperature and allowed to float against the top surface of a 200  $\mu\text{m}$  cellulose capillary tube (Spectrum Laboratories, Rancho Dominguez, CA, USA). Optical images from an upright microscope (BXFM, Olympus, Nederland BV, Zoeterwoude, The Netherlands), with a 60 $\times$  magnification objective (LUMFPL, Olympus; NA = 1.00, water immersion) and a 4 $\times$  magnifier (U-CA, Olympus) were captured by the Brandaris-128 camera as described previously in Ref. 17. Each recording contained 128 frames captured at  $13 \times 10^6$  frames per second, allowing the radial oscillations from a six cycle 1.6 MHz pulse to be measured. To demonstrate the mechanism of quasi-stable lipid shedding, Fig. 1(a) shows eight non-consecutive frames from a recording of a microbubble during the compression phase of one cycle of a 300 kPa peak negative pressure pulse. The bubble can be seen to fragment in frame 4, and shedding of a lipid bubble is observed. Initial resting radius of the microbubble was  $R_0 = 4.8 \mu\text{m}$ , which was reduced to  $R_0 = 3.5 \mu\text{m}$  at the end of

<sup>a)</sup>Author to whom correspondence should be addressed. Electronic mail: d.h.thomas@ed.ac.uk.

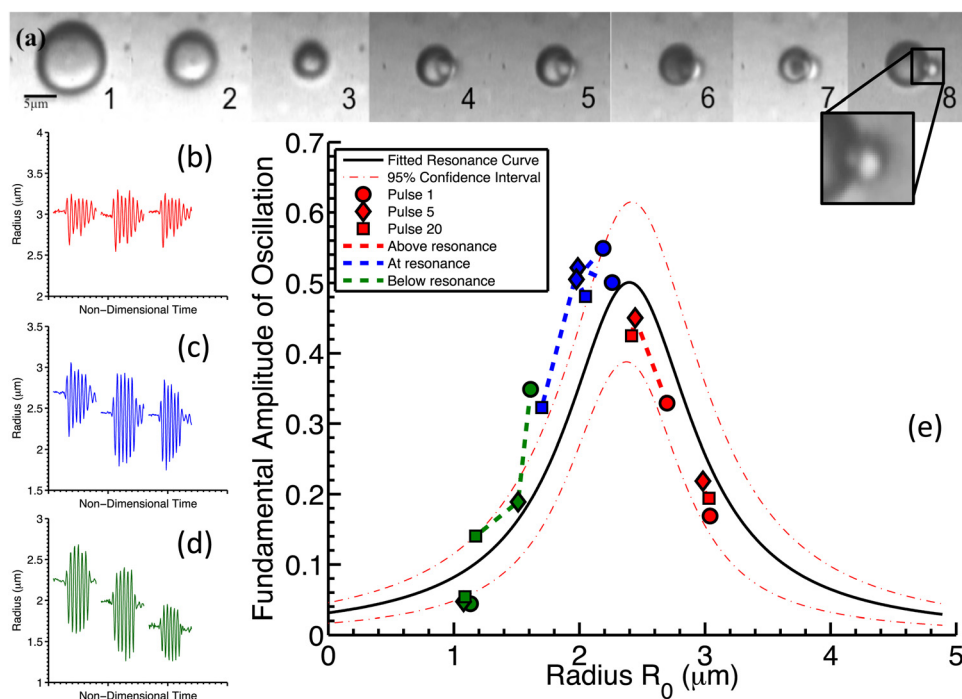


FIG. 1. (a) Sequence of 8 frames with inter-frame time of 152 ns taken from the Brandaris camera, showing the compression phase of oscillation, in response to an incident pulse of 300 kPa. The bubble can be seen to fragment in frame 4, and shedding of a small lipid bubble is observed. Initial resting radius was  $R_0 = 4.8 \mu\text{m}$ , and the final resting radius  $R_0 = 3.5 \mu\text{m}$ . The  $R_0 = 3.5 \mu\text{m}$  microbubble was observed to remain spherical and stable after the insonation. At lower pressures, this loss of shell material is not visible. (b)–(d) Radial oscillations of three microbubbles in response to non-consecutive 1.7 MHz 100 kPa pulses (1st, 5th, and 20th pulse are shown, with 80 ms between pulses). Initial radii are (b) above resonance  $R_0 = 3.0 \mu\text{m}$ , (c) approximately at resonance  $R_0 = 2.7 \mu\text{m}$ , and (d) above resonance  $R_0 = 2.2 \mu\text{m}$ . At the end of each of these three oscillations, a reduction in radii of (a) 0.1  $\mu\text{m}$ , (b) 0.3  $\mu\text{m}$  and (c) 0.8  $\mu\text{m}$  had occurred. No reduction in radius was observed between oscillations. (e) The respective change in microbubble radius of six microbubbles ( $R_0$ ), and how the fundamental amplitude of oscillation is affected in each case. Also plotted is the fitted resonance curve from 43 microbubble's 1st pulse responses (dashed line), with 95% confidence interval shown (faded dashed line). Microbubble decay follows a “controlled path” on the resonance curve, suggesting microbubbles which have reduced in radius behave as if insonated for the first time.

the oscillation, and the microbubble was observed to remain spherical and stable after the insonation. This figure shows that microbubbles can lose a significant amount of shell material to produce a subsequently stable microbubble. However, as 300 kPa incident pulses are above the fragmentation threshold and oscillations are likely to be non-spherical. In order to characterise the effect of shedding on the oscillation amplitude, subsequent optical measurements are performed at acoustic pressures below the fragmentation threshold.

43 single Definity microbubbles were insonated with consecutive pulses of six cycle 100 kPa peak negative pressure every 80 ms. Microbubbles were observed to reduce in radius by up to 15% in response to a total of 64 insonations over a total of 2.55 s. Following each reduction in radius, it was observed that the subsequent bubbles remained spherical and optically resembled those of a similar size but previously not insonated. The reductions in radius occurred during the insonations, and no significant reduction in radius occurred between insonations. Figures 1(b)–1(d) show examples of optical observations of three individual lipid shelled microbubbles, which demonstrate the stages of microbubble deflation. Incident pulses can be seen to produce stable and spherical oscillations, allowing the component of the radial oscillation corresponding to the fundamental frequency of the pulse,  $A_{\text{fun}}$ , to be calculated at different time points of the microbubble's deflation.<sup>18</sup> Fig. 1 shows oscillations from microbubbles that are initially above resonance (b), at resonance (c), and below resonance (d), with resonance radius ( $R_{\text{res}}$ ) defined as

that which gives maximum amplitude of oscillation. The resonance radius of the first insonation agrees with previous investigations of similar lipid shelled microbubbles.<sup>19,20</sup> The amplitudes of subsequent oscillations do not provide a significant departure from the resonance curve as calculated from the microbubble's first pulse response, and shown in Fig. 1(e). The data from 43 microbubble's first pulse responses have been fitted with a nonlinear least squares fit, and the 95% confidence interval is shown in Fig. 1(e). The majority of subsequent responses are contained within this interval. Microbubbles larger than the resonant radius ( $R_0 > 2.5 \mu\text{m}$ ) show an increase in amplitude of oscillation in response to subsequent oscillations and tend towards the mean resonance curve with each reduction in size. Microbubbles below the resonance peak ( $1 \mu\text{m} < R_0 < 2.5 \mu\text{m}$ ) have decreasing amplitude of oscillation with each radius reduction. Microbubbles with  $R_0 < 1 \mu\text{m}$  size show no observable oscillations above the resolution limit of the system.

A comparison between theory and experiment may help reveal the mechanism associated with the “quasi-stable” state of microbubbles resulting from exposure to consecutive ultrasound pulses. Under the influence of normal diffusion processes, a 10  $\mu\text{m}$  uncoated air bubble would dissolve in 1.17 s in a degassed water solution.<sup>21</sup> We have shown previously that the lipid shelled Definity<sup>®</sup> microbubbles used here will take much longer to dissolve due to the less soluble gas and the encapsulating lipid shell.<sup>22</sup> Thus changes in the scattered signal due to diffusion would be expected to be

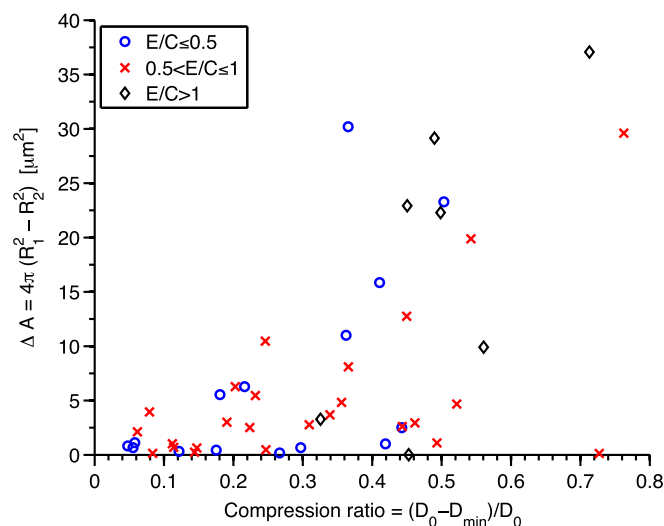


FIG. 2. Calculated loss of area from 32 microbubble radial oscillations, which show radius reductions from 1% to 15%. Change in area  $\Delta A$  has been plotted against relative compression ratio ( $C = D_0 - D_{\min}/D_0$ ), with signals classified by their expansion to compression ratio ( $E/C$ ), where  $E = (D_{\max} - D_0)/D_0$ .

insignificant over the 1 ms that separates the two ultrasound exposures in the experiments. Similarly the effects of gas diffusion on the bubble radius during insonation have also been shown to be negligible. Previous optical measurements on a lipid shelled agent over a similar time scale have shown that a single  $10 \mu\text{m}$  bubble will, however, reduce in radius<sup>15</sup> and the shell has been observed to deform before subsequently returning to a stable spherical state. It was proposed in this study that these observations were due to lipid shedding.

Microbubbles that are reduced in size in response to consecutive insonations are associated with an initial approximately spherical oscillation. Subsequent responses are also spherical, but occur at reduced radius as observed in Fig. 1. This supports the above suggestion of shedding of shell material. The subsequent change in radius  $\Delta R = R_{01} - R_{02}$  and loss in shell material area  $\Delta A = 4\pi(R_{01}^2 - R_{02}^2)$  has been calculated for each microbubble measured. If we assume that the area density of lipid remains approximately constant through sequential insonations, then the area of lost shell material will be directly proportional to the shell volume or mass. The mechanism of this loss of shell material is currently not fully understood, but it is shown here that this evolution occurs with the maintenance of sphericity.

Fig. 2 shows that the reduction in area  $\Delta A$  calculated from 32 stable microbubble oscillations significantly correlates ( $r = 0.6$ ) with the relative amount of compression the bubble undergoes, where  $C = (D_0 - D_{\min})/D_0$ . The range of change in radial amplitude is between 1% and 15%, with the larger changes occurring at resonance where the largest amplitudes of oscillation occur. Assuming size reduction occurs with the maintenance of sphericity, microbubble disruption is likely to be associated with excess lipid shedding in order to maintain consistent tension in the bubble shell.<sup>15</sup> The data shown in Fig. 2 show a significant correlation between the amount of compression a bubble undergoes and the subsequent amount of shell material shedding. Increased amounts of compression lead to an increased likelihood that

the bubbles will undergo shedding. Bubble signals are grouped by their relative expansion to compression ( $E/C$ ) ratio, where relative expansion  $E = (D_{\max} - D_0)/D_0$ , as previously defined by Ref. 23, into three categories:  $E/C \leq 0.5$ ,  $0.5 < E/C \leq 1$ , and  $E/C > 1$ . Although bubbles of all three categories are present above compression ratios of  $C > 0.4$ , the lack of expansion dominated signals ( $E/C > 1$ ) with both small amount of compression and large amounts of deflation suggests that compression is the dominant parameter for reduction in area. This data suggests there is a compression threshold below which the lipid shell is able to resist monolayer collapse or else recover from small amounts of collapse without loss of material. This may be related to low amplitude oscillations containing inadequate mechanical force to eject material.

The microbubbles investigated here are floating against the wall of a tube, which has previously been shown to produce asymmetric oscillations.<sup>20</sup> By comparing our settings with Vos *et al.*<sup>20</sup> we can conclude that the microbubble oscillations here present small asymmetries, and are thus relevant to targeted microbubble applications that are attached to a cell membrane or other surface and exposed to similar ultrasound fields. The experiments here were carried out at room temperature, which is well below the range of temperatures ( $42\text{--}55^\circ\text{C}$ ) at which a phase transition would be expected to take place.<sup>14</sup> However, previous experiments<sup>20,24</sup> have shown that lipid shelled microbubbles may undergo expansion at body temperature and show increased relative radial excursions upon insonation, both effecting their survival. *In-vitro* measurements made at room temperature, such as those presented here, therefore require careful interpretation with regard to behaviour *in-vivo*.

The data here present evidence that suggest that a mechanism of shell material shedding takes place at acoustic pressures below the microbubble fragmentation threshold, and that this mechanism can be reproducibly controlled. This mechanism may be studied further with the use of fluorescence imaging. This “quasi-stability” may be treated as a memory effect and help optimise signal processing algorithms to further improve the sensitivity of ultrasound contrast imaging. In addition, the controlled loss of shell material may be the subject of future drug delivery investigations. In particular where therapeutic materials are bound to the outside of the microbubble,<sup>25</sup> this mechanism of shell degradation requires better understanding to ensure efficiency in delivery to a target site. The potential for formation of new encapsulated structures from shed lipid and the implications for drug uptake will also require further investigation.

<sup>1</sup>J. R. Lindner, *Nat. Rev. Drug Discovery* **3**, 527 (2004).

<sup>2</sup>V. Sboros and M.-X. Tang, *Proc. Inst. Mech. Eng. Part H: J. Eng. Med.* **224**, 273 (2010).

<sup>3</sup>S. B. Feinstein, J. Cheirif, F. J. Ten Cate, P. R. Silverman, P. A. Heidenreich, C. Dick, R. M. Desir, W. F. Armstrong, M. A. Quinones, and P. M. Shah, *J. Am. Coll. Cardiol.* **16**, 316 (1990).

<sup>4</sup>G. M. Lanza, K. D. Wallace, M. J. Scott, W. P. Cacheris, D. R. Abendschein, D. H. Christy, A. M. Sharkey, J. G. Miller, P. J. Gaffney, and S. A. Wickline, *Circulation* **94**, 3334 (1996).

<sup>5</sup>L. J. M. Juffermans, P. A. Dijkman, R. J. P. Musters, C. A. Visser, and O. Kamp, *Am. J. Physiol. Heart Circ. Physiol.* **291**, H1595 (2006).

<sup>6</sup>Y. Taniyama, K. Tachibana, K. Hiraoka, T. Namba, K. Yamasaki, N. Hashiya, M. Aoki, T. Ogihara, K. Yasufumi, and R. Morishita, *Circulation* **105**, 1233 (2002).

- <sup>7</sup>C. R. Anderson, X. Hu, J. Tlaxca, A.-E. Decleves, R. Houghtaling, K. Sharma, M. Lawrence, K. Ferrara, and J. J. Rychak, *Invest. Radiol.* **46**, 215 (2011).
- <sup>8</sup>E. Stride and N. Saffari, *Ultrasound Med. Biol.* **29**, 563 (2003).
- <sup>9</sup>J. E. Chomas, P. Dayton, J. Allen, K. Morgan, and K. W. Ferrara, *IEEE Trans. Ultrason. Ferroelectr. Freq. Control* **48**, 232 (2001).
- <sup>10</sup>A. Bouakaz, M. Versluis, and N. de Jong, *Ultrasound Med. Biol.* **31**, 391 (2005).
- <sup>11</sup>V. Sboros, *Adv. Drug Delivery Rev.* **60**, 1117 (2008).
- <sup>12</sup>P. Marmottant, S. van der Meer, M. Emmer, M. Versluis, N. de Jong, S. Hilgenfeldt, and D. Lohse, *J. Acoust. Soc. Am.* **118**, 3499 (2005).
- <sup>13</sup>P. Marmottant, A. Bouakaz, N. de Jong, and C. Quilliet, *J. Acoust. Soc. Am.* **129**, 1231 (2011).
- <sup>14</sup>G. Pu, M. A. Borden, and M. L. Longo, *Langmuir* **22**, 2993 (2006).
- <sup>15</sup>M. A. Borden, D. E. Kruse, C. F. Caskey, S. Zhao, P. A. Dayton, and K. W. Ferrara, *IEEE Trans. Ultrason. Ferroelectr. Freq. Control* **52**, 1992 (2005).
- <sup>16</sup>F. Guidi, H. J. Vos, R. Mori, N. de Jong, and P. Tortoli, *IEEE Trans. Ultrason. Ferroelectr. Freq. Control* **57**, 193 (2010).
- <sup>17</sup>C. T. Chin, C. Lancée, J. Borsboom, F. Mastik, M. E. Frijlink, N. de Jong, M. Versluis, and D. Lohse, *Rev. Sci. Instrum.* **74**, 5026 (2003).
- <sup>18</sup>S. M. van der Meer, B. Dollet, M. M. Voormolen, C. T. Chin, A. Bouakaz, N. de Jong, M. Versluis, and D. Lohse, *J. Acoust. Soc. Am.* **121**, 648 (2007).
- <sup>19</sup>M. Emmer, A. Vanwamel, D. Goertz, and N. de Jong, *Ultrasound Med. Biol.* **33**, 941 (2007).
- <sup>20</sup>H. J. Vos, B. Dollet, J. G. Bosch, M. Versluis, and N. de Jong, *Ultrasound Med. Biol.* **34**, 685 (2008).
- <sup>21</sup>A. A. Doinikov, L. Aired, and A. Bouakaz, *Phys. Med. Biol.* **56**, 6951 (2011).
- <sup>22</sup>V. Sboros, C. Moran, T. Anderson, and W. McDicken, *Ultrasound Med. Biol.* **26**, 807 (2000).
- <sup>23</sup>N. de Jong, M. Emmer, C. T. Chin, A. Bouakaz, F. Mastik, D. Lohse, and M. Versluis, *Ultrasound Med. Biol.* **33**, 653 (2007).
- <sup>24</sup>H. Mulvana, E. Stride, J. V. Hajnal, and R. J. Eckersley, *Ultrasound Med. Biol.* **36**, 925 (2010).
- <sup>25</sup>I. Lentacker, B. Geers, J. Demeester, S. C. De Smedt, and N. N. Sanders, *Mol. Ther.* **18**, 101 (2010).